Chapter 2
Thermodynamics of Physical and Chemical Vapour Deposition

The ultimate goal of this chapter is to formulate the driving force for deposition of diamond in the chemical vapour deposition. Before reaching that goal, we will study the basics of the related topics in several steps. First, we will study how to formulate the thermodynamics of ideal gases. Then we will study how to formulate the driving force for evaporation and condensation of water, which we experience during our everyday lives, such as drying wet clothes and mist formation. Then, we will study how we formulate the driving force for deposition in the physical vapour deposition process. In the next step, we will study how to formulate the irreversibility when chemical reactions are involved. Finally, we will study how to formulate the driving force for deposition in the CVD process. At the end of the chapter, some kinetic concept will be briefly described. The motivation for formulating the driving force for deposition was to compare the nucleation curves between diamond and graphite. This allows us to compare not only the stability but also the activation energy for nucleation between diamond and graphite.

2.1 Ideal Gases

For a closed system of fixed composition at constant temperature, dG becomes (Gaskell 1995)

$$dG = VdP \tag{2.1}$$

Since V = RT/P for one mole of ideal gas,

$$dG = \frac{RT}{P}dP = RTd\ln P \tag{2.2}$$

For an isothermal change of pressure from P_1 to P_2 at T,

N.M. Hwang, *Non-Classical Crystallization of Thin Films and Nanostructures in CVD and PVD Processes*, Springer Series in Surface Sciences 60,
DOI 10.1007/978-94-017-7616-5_2

$$G(P_2, T) - G(P_1, T) = RT \ln \frac{P_2}{P_1} \tag{2.3}$$

$$G(P, T) = G(P_o, T) + RT \ln \frac{P}{P_o} \tag{2.4}$$

where $G(P_o,T)$ is a reference state. Since the choice of a reference state is arbitrary, it would be good if we make a convenient choice. If the reference state is chosen as P_o = 1 atm at the given temperature, (2.4) is simplified to

$$G = G^o + RT \ln P \tag{2.5}$$

Due to the simplicity of (2.5), this special reference state is called the standard state, which is defined by the state of 1 mol of pure gas at 1 atm pressure and the temperature of interest.

The chemical potential of pure gas is equal to the molar free energy. Therefore, (2.5) can also be written as

$$\mu = \mu^o + RT \ln P \tag{2.6}$$

However, the chemical potential of a component A in a mixture gas is equal to the partial molar Gibbs free energy, which is written as

$$\bar{G}_A = G_A^o + RT \ln p_A \tag{2.7}$$

where p_A is the partial pressure of the component A in the mixture gas.

And the corresponding chemical potential is

$$\mu_A = \mu_A^o + RT \ln p_A \tag{2.8}$$

(Q) What would be the driving force for wet clothes to dry?

2.2 Driving Force for Evaporation

The evaporation process is the irreversible transfer of atoms or molecules from the liquid to the gas phase. Water will evaporate when its chemical potential of the liquid is higher than that of the gas phase. This can be expressed as

$$\Delta\mu_{H_2O}^{liquid \rightarrow gas} = \mu_{H_2O}^{gas} - \mu_{H_2O}^{liquid} \tag{2.9}$$

If it is assumed that the water vapour follows the ideal gas behaviour, the chemical potential of water in the gas phase is expressed as

$$\mu_{H_2O,gas} = \mu^o_{H_2O,gas} + RT \ln p_{H_2O} \tag{2.10}$$

where p_{H_2O} is the vapour pressure of water in the gas phase. Then, what remains to do is to determine the chemical potential of water.

As in (2.1), the molar free energy or the chemical potential of liquid water can be expressed at the given temperature as

$$d\mu = VdP \tag{2.11}$$

The molar volume of liquid is insensitive to the change of pressure, (2.11) can be integrated with respect to P.

$$\mu(P,T) = \mu(P_o,T) + V(P - P_o) \tag{2.12}$$

If the reference state is defined as the pure water at 1 atm pressure and the temperature of interest, which is identical to the standard state, (2.12) can be written as,

$$\mu_{H_2O,liquid} = \mu^o_{H_2O,liquid} + V(P - 1) \tag{2.13}$$

Since the molar volume of liquid is much smaller than that of gas, the term V (P − 1) is negligibly small compared with the chemical potential of the standard state. So (2.13) can be safely approximated as

$$\mu_{H_2O,liquid} = \mu^o_{H_2O,liquid} \tag{2.14}$$

The approximation in (2.14) is valid for most condensed phases unless the pressure is very high.

The chemical potential in (2.14) cannot be directly compared with that in the gas phase in (2.10) because the reference state is different. For comparison, the same reference state should be used. If the standard state for gas is used as a reference state, (2.14) can be written as

$$\mu_{H_2O,liquid} = \mu^o_{H_2O,gas} + RT \ln p^{eq}_{H_2O} \tag{2.15}$$

where $P^{eq}_{H_2O}$ is the equilibrium vapour pressure of water at the given temperature.

If (2.10) and (2.15) are substituted in (2.9),

$$\Delta\mu^{liquid \to gas}_{H_2O} = \mu^o_{H_2O,gas} + RT \ln p_{H_2O} - \mu^o_{H_2O,gas} - RT \ln p^{eq}_{H_2O} = RT \ln \left(\frac{p_{H_2O}}{p^{eq}_{H_2O}} \right) \tag{2.16}$$

which can also be written as

$$\Delta\mu_{H_2O}^{liquid\rightarrow gas} = -RT\ln\left(\frac{p_{H_2O}^{eq}}{p_{H_2O}}\right) \tag{2.17}$$

If the relative humidity is 50 %, the value in the parenthesis is 2 and the driving force for evaporation would be

$$\Delta\mu_{H_2O}^{liquid\rightarrow gas} = -RT\ln 2 \tag{2.18}$$

The ratio in the parenthesis in (2.17) is defined as the supersaturation ratio for evaporation.

(Q) What would be the driving force for precipitation of water when the water vapour, which was saturated at 300 K, is suddenly supercooled to 290 K?

2.3 Driving Force for Condensation

In this process, the water molecule is transferred from the vapour to the liquid state. Using the similar scheme above, the driving force can be written as

$$\Delta\mu_{H_2O}^{gas,300K\rightarrow liquid,290K} = \mu_{H_2O}^{liquid,290K} - \mu_{H_2O}^{gas,300K} \tag{2.19}$$

$$= \mu_{H_2O,gas}^{o} + RT\ln p_{H_2O}^{290K} - \left(\mu_{H_2O,gas}^{o} + RT\ln p_{H_2O}^{300K}\right) \tag{2.20}$$

where $P_{H_2O}^{290K}$ and $P_{H_2O}^{300K}$ represent the equilibrium vapour pressure of water respectively at 290 and 300 K.

The driving force for condensation becomes

$$\Delta\mu^{300K\rightarrow 290K} = -RT\ln\left(\frac{P_{H_2O}^{300K}}{P_{H_2O}^{290K}}\right) \tag{2.21}$$

The ratio of the parenthesis is called the supersaturation ratio for condensation.

2.4 Driving Force for Deposition in the Physical Vapour Deposition Process

In the physical vapour deposition (PVD) process, the materials to be deposited are evaporated thermally or by sputtering. The species in the vapour state are supersaturated for condensation or precipitation. Therefore, the PVD process consists of

evaporation and condensation. When the metal evaporates at equilibrium vapour pressure of P^{eq} at temperature T with the ambient hydrostatic pressure P of the evaporant vapour, the evaporation flux is expressed by the Hertz-Knudsen equation as

$$J = \frac{\alpha_e(P^{eq} - P)}{\sqrt{2\pi mkT}} \quad \text{mols/s cm}^2 \tag{2.22}$$

where α_e is the evaporation coefficient for vapour molecules onto the surface. The evaporation coefficient is usually much less than unity because the evaporant vapour molecules impinging upon the condensed phase surface are reflected back.

Since the mass of the evaporated flux is conserved, the number density of the evaporated molecules decrease along with the distance from the evaporation source. If the evaporation source is a point, the number density decreases with distance, being inversely proportional to the square distance. If the evaporation source is an infinite line, the number density decreases, being inversely proportional to the distance. In the steady state, a certain pressure P will be maintained in the vicinity of the growing surface. This pressure will be in equilibrium with the adatoms on the growing surface or substrate. If this pressure is denoted as P^* and the equilibrium vapour pressure of the evaporant at the substrate temperature is P^{eq}_{Tsub}, the supersaturation ratio for deposition is given as

$$\alpha = \frac{P^*}{P^{eq}_{Tsub}} \tag{2.23}$$

And the driving force for deposition is given as

$$\Delta\mu = -RT \ln \alpha \tag{2.24}$$

(Q) In the chemical vapour deposition, chemical reactions are involved. How can you formulate the irreversibility of chemical reactions? What would be the driving force for chemical reactions?

2.5 Irreversibility for Chemical Reactions

Consider the chemical reaction where gases A and B react with each other and produce gas 2C (Gaskell 1995). Initially there are 1 mol of A and 1 mol of B with C being absent. If 2x mole of C is formed by chemical reaction after time t, the number of moles of both A and B would be 1 – x as shown by the following equation.

$$\begin{array}{llll} & A_{(g)} + B_{(g)} \Leftrightarrow & 2C_{(g)} & \\ \text{at t = 0,} & 1 & 1 & 0 \\ \text{at t = t,} & 1 - x & 1 - x & 2x \end{array} \tag{2.25}$$

The Gibbs free energy of the system becomes

$$G' = (1-x)\mu_A + (1-x)\mu_B + 2x\mu_C = \mu_A + \mu_B + x(2\mu_C - \mu_A - \mu_B) \tag{2.26}$$

The derivative of G′ with respect to x can be positive, zero or negative. If the derivative is positive, the reaction to produce C would increase the Gibbs free energy of the system, which is not allowed. This means that the reaction would be backward. C is unstable and decomposes into B and C. The sum of chemical potential on the right hand side of the chemical reaction is larger than that on the left side.

$$\left(\frac{\partial G'}{\partial x}\right) = 2\mu_C - \mu_A - \mu_B > 0 \rightarrow \mu_A + \mu_B < 2\mu_C \tag{2.27}$$

If the derivative is zero, the chemical reaction is in equilibrium. The sum of chemical potential on the right hand side is equal to that on the left side.

$$\left(\frac{\partial G'}{\partial x}\right) = 2\mu_C - \mu_A - \mu_B = 0 \rightarrow \mu_A + \mu_B = 2\mu_C \tag{2.28}$$

If the derivative is negative, the reaction to produce C would decrease the Gibbs free energy, which is allowed. This means that the reaction would be forward. C is stable and would be formed at the expense of B and C. The sum of chemical potential on the right hand side of the chemical reaction is smaller than that on the left side.

$$\left(\frac{\partial G'}{\partial x}\right) = 2\mu_C - \mu_A - \mu_B < 0 \rightarrow \mu_A + \mu_B > 2\mu_C \tag{2.29}$$

This conclusion is generally valid for any chemical reaction. If the sum of chemical potentials on the left side is larger than that on the right side, the forward reaction will be irreversible. If the sum of chemical potentials on the left side is smaller than that on the right side, the backward reaction will be irreversible. If the sum of chemical potentials on the left side is equal to that on the right side, the chemical reaction is in equilibrium.

If the reactants are on the left side and the products are on the right side, the driving force for the forward reaction can be written as

$$\Delta\mu = \sum \mu_i^p n_i^p - \sum \mu_i^r n_i^r \tag{2.30}$$

This driving force changes with time or the chemical reaction. Consider the simple reaction of (2.25).

$$\Delta\mu = 2\mu_C - \mu_A - \mu_B = 2\mu_C^o + 2RT\ln p_C - \mu_A^o - RT\ln p_A - \mu_B^o - RT\ln p_B \tag{2.31}$$

$$\Delta\mu = \Delta\mu^o + RT\ln\frac{p_C^2}{p_A p_B} \tag{2.32}$$

Since C is initially absent, P_C is equal to zero. Then the driving force in (2.32) becomes infinite. This infinite driving force comes from the entropy of mixing, which goes to infinity when something new is formed infinitesimally. This means that the driving force for existence from non-existence is infinite. In other words, nature tries to experience all the possible things it can.

The driving force for the chemical reaction in (2.32) continues to decrease as the reaction goes on until Δμ becomes zero, where the equilibrium state is reached. If the chemical reaction proceeds further, it will increase Δμ, which is not allowed by the second law of thermodynamics. Therefore, once the equilibrium is reached, the irreversible chemical reaction stops. However, the reversible chemical reaction continues, satisfying the constraint of the dynamic equilibrium that the rates of the forward and backward reactions are the same.

2.6 Driving Force for Deposition in the Chemical Vapour Deposition Process

Consider a chemical reaction similar to (2.25) but this time the component C is not gas but solid.

$$A_{(g)} + B_{(g)} \Leftrightarrow C_{(s)} \tag{2.33}$$

This reaction would be one example of chemical vapour deposition. The driving force for the forward reaction of (2.33) is expressed as

$$\Delta\mu = \Delta\mu^o + RT\ln\frac{1}{p_A p_B} \tag{2.34}$$

where $\Delta\mu^o$, p_A, and p_B are respectively standard chemical potential change (or standard molar Gibbs free energy change), partial pressure of A and partial pressure of B. It should be noted that since the chemical potential of the condensed phase is equal to that of its standard state, $p_C = 1$. Equation (2.34) represents the driving force for the forward chemical reaction, which should be distinguished from the driving force for deposition of C (Hwang and Yoon 1994a).

(Q) What would be the driving force for deposition of solid C as a result of the chemical reaction of (2.33)?

This question may not be easy to answer. It would be better to answer an easier question as follows. Consider the A–B binary alloy, where the α solid solution is stable at high temperature and the β solid solution is stable at low temperature. If the alloy of the composition $X_B^{\alpha_o}$ is supercooled from the α one phase region into the two phase region of α + β, the α phase will be decomposed as follows.

$$\alpha \rightarrow \alpha' + \beta \tag{2.35}$$

(Q) What would be the driving force for precipitation of β?

In Fig. 2.1, the molar Gibbs free energies of the α and β phases for the A–B alloy are shown with respect to X_B. The final equilibrium state of α′ + β is defined by the common tangent $\overline{QS}$. The molar Gibbs free energy at the composition $X_B^{\alpha_o}$ in the equilibrium state is denoted as R. And the driving force for the reaction of (2.35) is $\overline{OR}$ in Fig. 2.1. However, this driving force should be distinguished from the driving force for precipitation of β. The driving force $\overline{OR}$ is dissipated in the decomposition of α into α′ and β. However, we do not use this value as a driving force for nucleation of β. In other words, this driving force is not used to calculate the critical nucleus or the nucleation barrier of β. The driving force for precipitation of β should be evaluated at the composition of β, which is $X_B^{\beta_o}$ in Fig. 2.1. The molar Gibbs free energy of β at $X_B^{\beta_o}$, which is $G_m^{\beta}\left(X_B^{\beta_o}\right)$, is designated as Q in Fig. 2.1. At the composition of $X_B^{\beta_o}$, we need to determine the Gibbs free energy of the state which is supersaturated with respect to precipitation of β. This supersaturated state should be in equilibrium with the initial state, which is the α phase at the composition of $X_B^{\alpha_o}$. The tangent on the molar Gibbs free energy curve of the α phase at $X_B^{\alpha_o}$ represents the molar Gibbs free energy of varying composition in equilibrium with the α phase at $X_B^{\alpha_o}$. For example, the intercept of the tangent at the axis of $X_B = 1$ represents $\mu_B^{\alpha}(X_B^{\alpha_o})$, which is the chemical potential of B in equilibrium with the α phase at $X_B^{\alpha_o}$. Likewise, the intercept of the tangent at the axis of

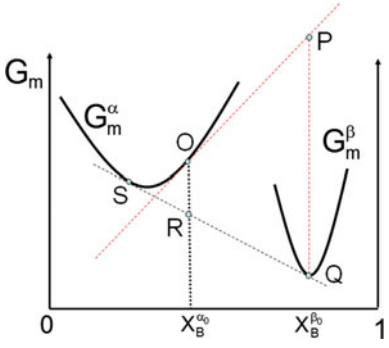

Fig. 2.1 Molar Gibbs free energy of α and β phases in the binary A–B alloy, illustrating the driving force for precipitation of β at $X_B^{\beta_o}$ from the α matrix at $X_B^{\alpha_o}$ (Hillert and Aaronson 1975)

$X_B = 0$ represents $\mu_A^{\alpha}(X_B^{\alpha_o})$, which is the chemical potential of A in equilibrium with the α phase at $X_B^{\alpha_o}$. Therefore, the molar Gibbs free energy at the composition of $X_B^{\beta_o}$ in equilibrium with the α phase at $X_B^{\alpha_o}$ is determined by the intercept of the tangent with the axis of $X_B = X_B^{\beta_o}$. This value is designated as P in Fig. 2.1. Therefore, the driving force for precipitation of β is $\overline{PQ}$ in Fig. 2.1. It should be noted that the driving force for precipitation of β changes as the composition of the α matrix changes with the precipitation process because the tangent should be made at the new composition of the α matrix.

With this thermodynamic scheme in mind, consider the driving force for deposition of the solid C in the chemical reaction of (2.33). It should be noted that the driving force should be evaluated at the composition of the solid C. The driving force should be the difference of the chemical potential of C between solid and gas. If the standard state for gas is used as a reference state, the chemical potential of C in solid, $\mu_{C,solid}$, is expressed as

$$\mu_{C,solid} = \mu^o_{C,gas} + RT \ln p_C^{eq} \tag{2.36}$$

where P_C^{eq} is the equilibrium vapour pressure of C at the substrate temperature.

Since the driving force for deposition is the difference in the chemical potential C between solid and gas in the vicinity of the growing film, the remaining problem is to identify the chemical potential of C in gas, $\mu_{C,gas}$, made by the chemical reaction of (2.33). If the steady state partial pressure of C in the vicinity of the growing film is denoted as $P_{C,gas}$, the driving force is expressed as

$$\Delta\mu_C^{gas\rightarrow solid} = \mu_{C,solid} - \mu_{C,gas} = \mu^o + RT\, ln\, p_C^{eq} - \mu^o - RT\, ln\, p_{C,gas} \tag{2.37}$$

Arranging (2.37) gives (Hwang and Yoon 1994a)

$$\Delta\mu_C^{gas\rightarrow solid} = -RT\, ln \frac{p_{C,gas}}{p_C^{eq}} \tag{2.38}$$

And $P_{C,gas}/P_C^{eq}$ is the supersaturation ratio α for deposition. To determine α or driving force for deposition, we need to determine $p_{C,gas}$. The steady state value of $p_{C,gas}$ in the CVD process depends on the kinetics of chemical reactions under the given processing conditions with temperature as a major factor. If plasma is used in the CVD process, it drastically increases the kinetics of chemical reactions.

Think about the extreme case where the chemical reaction of (2.33) hardly occurs in the CVD reactor. This would happen if the reactor temperature is too low to decompose the reactant gases. Then, there will be no deposition because $p_{C,gas}$ would be practically zero. $p_{C,gas}$ would increase with the extent of the chemical reaction. Depending on the extent of chemical reaction, $p_{C,gas}$ can have the three ranges of values as follows.

$$0 \leq p_{C,gas} < p_C^{eq} \tag{2.39}$$

$$p_{C,gas} = p_C^{eq} \tag{2.40}$$

$$p_C^{eq} < p_{C,gas} \leq p_{C,gas}^{max} \tag{2.41}$$

where $p_{C,gas}^{max}$ represents the maximum value that $p_{C,gas}$ can have. In the range of (2.39), the supersaturation ratio $\alpha = p_{C,gas} / p_C^{eq}$ is less than 1 and the driving force is for etching rather than for deposition. In (2.40), α is 1 and the driving force is zero, indicating neither deposition nor etching occurs. Only in the range of (2.41), α is larger than 1 and the driving force is for deposition.

(Q) How can $p_{C,gas}^{max}$ *be determined?*

$p_{C,gas}^{max}$ represents the partial pressure of C that is obtained by the maximum extent of reaction or the maximum metastable state without precipitating the solid. It can be determined by minimizing the Gibbs free energy excluding the condensed phase of C. In other words, $p_{C,gas}^{max}$ can be determined by minimizing the Gibbs free energy of the gas phase only (Hwang and Yoon 1994a). Therefore, the maximum supersaturation ratio and driving force can be expressed as

$$\alpha = p_{C,gas}^{max} / p_C^{eq} \tag{2.42}$$

$$\Delta\mu = -RT\, ln\left(p_{C,gas}^{max} / p_C^{eq}\right) \tag{2.43}$$

In the real practice of CVD, if $P_{C,gas} \ll P_{C,gas}^{max}$, most reactant gases flow out of the CVD reactor without undergoing an appreciable extent of chemical reactions, resulting in very low efficiency. Therefore, such a CVD condition would not be adopted. In most processes, process parameters would be adjusted to maximize the chemical reactions of reactants so that the condition of $P_{C,gas} \approx P_{C,gas}^{max}$ may be achieved. In this sense, $P_{C,gas} \approx P_{C,gas}^{max}$ may be a reasonable approximation. Since $P_{C,gas}^{max}$ can be determined by minimization of the Gibbs free energy of the gas phase only, $\alpha = p_{C,gas}^{max} / p_C^{eq}$ can be calculated with respect to thermodynamic parameters such as temperature, pressure and composition.

Equations (2.42) and (2.43) as a reasonable approximation can be used if the nucleation occurs in the gas phase. In most CVD processes, however, nucleation and growth are believed to occur on the substrate or surface. Besides, it is known that most flux contributing to the film growth does not directly come from the gas phase but come from the diffusion of adatoms on the surface. First, the gas atoms are adsorbed on the terrace. And then the adatoms diffuse to the ledge of monoatomic height. Since monoatomic ledges have abundant kinks, the adatoms will find kink sites, where they become incorporated into the crystal. This means that we

need to evaluate the supersaturation ratio in terms of the adatoms on the surface. The composition of the adsorbed species may be different from that of the gas phase because the desorption energies are different for each species.

(Q) How can you formulate the supersaturation ratio and the driving force for deposition on the surface?

2.7 Consideration of the Substrate or Surface

Considering the surface, $p^{max}_{C,gas}$ and p^{eq}_{C} in (2.42) should be replaced by the corresponding adsorbed concentrations. If the equilibrium between the gas phase and the surface is maintained, the ratio in (2.42) does not change and thus (2.43) does not change because the chemical potentials of the species in the gas phase are the same as those on the adsorbed species. If the process is in the steady state, it is safely assumed that the equilibrium between the gas and the surface is maintained. If the equilibrium between the gas phase and the surface is not maintained, the adsorbed concentration may not be in the steady state but depend on time. Then, the supersaturation ratio and the driving force are different from (2.42) and (2.43) respectively. In such a non-steady state, it is difficult to determine the superstation ratio and the driving force.

When the species to be deposited is a compound or a solid solution by the CVD process, the partial pressure or the equilibrium vapour pressure is often difficult to define. For example, compounds such as SiC, SiO_2 and Si_3N_4, do not have vapour species corresponding to the same stoichiometry of the solid phase.

(Q) How can you formulate the supersaturation ratio and the driving force for deposition of compounds or solid solution?

2.8 Driving Force for Deposition of Compound or Solid Solution

The compound A_aB_b does not have the vapour species of the same stoichiometry, where A and B are the element. If (2.42) is applied, the supersaturation ratio for deposition of A_aB_b is expressed as

$$\alpha = \frac{p^{max}_{A_aB_b,gas}}{p^{eq}_{A_aB_b}} \tag{2.44}$$

The problem is that $p^{max}_{A_aB_b,gas}$ and $p^{eq}_{A_aB_b}$ cannot be determined because the compound A_aB_b does not exist in the gas phase. However, the ratio of $p^{max}_{A_aB_b,gas}$ to $p^{eq}_{A_aB_b}$ can be determined by considering the gas species that are in equilibrium with the

hypothetical gas compound A_aB_b. Consider the two hypothetical equilibria: one for the metastable gas phase equilibrium and the other for the stable equilibrium.

$$aA^{gas,eq} + bB^{gas,eq} = A_aB_b^{gas,eq} \tag{2.45}$$

$$aA^{eq} + bB^{eq} = A_aB_b^{eq} \tag{2.46}$$

From these two equilibria of (2.45) and (2.46), the following relationship is derived.

$$\alpha = \frac{p_{A_aB_b,gas}^{max}}{p_{A_aB_b}^{eq}} = \frac{\left(p_{A,gas}^{max}\right)^a \left(p_{B,gas}^{max}\right)^b}{\left(p_A^{eq}\right)^a \left(p_B^{eq}\right)^b} \tag{2.47}$$

And $p_{A,gas}^{max}$, $p_{B,gas}^{max}$, p_A^{eq} and p_B^{eq} can be determined by the metastable gas phase equilibrium and the stable equilibrium of the chemical reaction. From (2.47), the driving force for deposition can also be determined. (Hwang and Yoon 1994b)

This result can be extended to the solid solution by assuming that the stoichiometry coefficients a and b can continuously change within the solid solution range with the constraint of a + b = 1, which is needed when the driving force is evaluated per mole of the solid solution.

Let's take an example of SiC deposition using the reactant gases of SiH_4 and CH_4. The overall chemical reaction would be as follows.

$$SiH_4 + CH_4 = SiC + 4H_2 \tag{2.48}$$

If the thermodynamic scheme of (2.47) is applied to the reaction in (2.48), the supersaturation ratio is expressed as

$$\alpha = \frac{p_{SiC,gas}^{max}}{p_{SiC}^{eq}} = \frac{p_{SiH_4,gas}^{max} p_{CH_4,gas}^{max} \left(p_{H_2}^{eq}\right)^4}{p_{SiH_4}^{eq} p_{CH_4}^{eq} \left(p_{H_2,gas}^{max}\right)^4} \tag{2.49}$$

The supersaturation ratio can be expressed in a more simplified form by considering a following reaction satisfying the law of mass action.

$$Si + C = SiC \tag{2.50}$$

If the thermodynamic scheme in (2.47) is applied to (2.50), the supersaturation ratio is expressed as

$$\alpha = \frac{p_{SiC,gas}^{max}}{p_{SiC}^{eq}} = \frac{p_{Si,gas}^{max} p_{C,gas}^{max}}{p_{Si}^{eq} p_C^{eq}} \tag{2.51}$$

which is much simpler than (2.49)

2.9 Calculation Examples Using Thermo-Calc

2.9.1 Si–Cl–H System

At the temperature of 1323 K and the pressure of 10,666 Pa with the gas mixture of SiH_4 : HCl : H_2 = 0.14 : 0.92 : 99, the following conditions are set for calculation by Thermo-Calc (Sundman et al. 1985).

Set-Conditions: T = 1323, P = 10,666, N(Si) = 1.4E–1, N(Cl) = 9.2E–1, N(H) = 199.36

Here, N represents the number of moles. The Gibbs free energy minimization under these conditions produces the following amount of solid silicon and gases. Here, SI1, which has a mole fraction of 7.97411E–10, corresponds to the equilibrium vapour pressure of silicon at the given temperature.

H2	9.91047E–01	CL2H2SI1	3.78938E–06	SI1	7.97511E–10
CL1H1	8.72066E–03	CL4SI1	7.88797E–07	CL2	5.88841E–13
CL2SI1	2.12707E–04	H4SI1	8.60203E–08	SI2	2.60034E–13
CL3SI1	5.55192E–06	CL1	3.56902E–08	SI3	3.14674E–14
H1	4.83980E–06	CL1SI1	9.72339E–09	H6SI2	6.50693E–15
CL3H1SI1	4.57379E–06	H1SI1	2.01285E–09		

SI1_S#1			Status ENTERED	Driving force	0.0000E+00
Number of moles		1.1722E–01	Mass 3.2921E+00	Mole fraction	
SI	1.00000E+00	CL	0.00000E+00	H	0.00000E+00

The Gibbs free energy minimization by suspending condensed phases of silicon in the calculations produces the following amount of gases. Here, SI1, which has a mole fraction of 9.40131E−10, corresponds to the maximum partial pressure of silicon in the supersaturated gas phase, where condensed phases of silicon did not precipitate.

H2	9.92254E−01	H1	4.84275E−06	SI1	9.40131E−09
CL1H1	6.34253E−03	CL4SI1	2.59578E−06	SI3	5.15678E−11
CL2SI1	1.32491E−03	H4SI1	1.01663E−06	SI2	3.61445E−11
CL3SI1	2.51360E−05	CL1SI1	8.33246E−08	H6SI2	9.07768E−13
CL2H2SI1	2.36321E−05	CL1	2.59417E−08	CL2	3.11097E−13
CL3H1SI1	2.07202E−05	H1S1	2.37455E−08		

The supersaturation ratio for deposition of Si can be determined as

$$\alpha = \frac{p_{Si}^{\max}}{p_{Si}^{eq}} = \frac{9.40131 \times 10^{-9}}{7.97411 \times 10^{-10}} = 11.79$$

2.9.2 Si–C–H System

At the temperature of 1400 K and the pressure 1000 Pa with the gas mixture of $SiH_4 : CH_4 = 1 : 1$, the following conditions are set for calculation by Thermo-Calc (Sundman et al. 1985).

Set-Conditions: T = 1400, P = 1000, N(Si) = 1, N(C) = 1, N(H) = 8

The Gibbs free energy minimization under these conditions produces the following.

H2	9.99951E−01	C2H4	3.00948E−13	C3H4_1	1.09232E−19
H	4.87045E−05	C1H2	6.00656E−15	C	1.05200E−19
C1H4	1.64031E−07	C2H3	1.17540E−15	C3H6_2	1.59231E−21
SI	9.98049E−08	C2SI1	1.02915E−15	C3H6_1	2.53376E−24
H1SI1	5.25792E−08	H6SI2	1.31302E−16	C2	1.05475E−24
H4SI1	1.16175E−08	C2H6	5.95508E−17	C3	2.51092E−25
C1H3	1.67072E−10	C2H1	1.49582E−17	C3H8	5.92461E−26
SI2	8.01027E−11	C1SI1	6.96977E−18	C4	1.00000E−30
C1SI2	6.87487E−11	C2H5	2.43303E−18	C4H12SI1	1.00000E−30
C2H2	3.82934E−11	C1H1	1.39138E−18	C5	1.00000E−30
SI3	1.48834E−11	C3H4_2	3.16405E−19		

The Gibbs free energy minimization by suspending all condensed phases related to silicon, carbon and silicon carbide in the calculations produces the following amount of gases.

H2	8.30213E−01	C1H3	5.15943E−06	C1SI1	5.66556E−11
C1SI2	1.11284E−01	C3H4_1	5.12173E−06	C3	1.70796E−11
C1H2	5.29783E−02	SI2	3.17637E−06	H6SI2	2.97979E−12
C1H4	4.61561E−03	H4SI1	1.59469E−06	C3H8	1.91491E−12
C2H4	3.45682E−04	C2H3	1.48171E−06	C5	5.42009E−13
C2SI1	3.41494E−04	C3H6_2	6.19877E−08	C1H1	5.17529E−14
SI3	1.17524E−04	C2H6	5.67915E−08	C	4.29435E−15
H	4.43787E−05	C2H1	2.27117E−08	C4	2.46159E−15
SI	1.98744E−05	C2H5	2.54647E−09	C2	1.75758E−15
C3H4_2	1.48358E−05	C1H2	2.03572E−10	C4H12SI1	5.68974E−16
H1SI1	9.54028E−06	C3H6_1	9.86377E−11		

If the supersaturation ratio for deposition of silicon carbide is calculated based on (2.49)

$$\alpha_1 = \frac{p^{max}_{SiC,gas}}{p^{eq}_{SiC}} = \frac{p^{max}_{SiH_4,gas}\, p^{max}_{CH_4,gas} \left(p^{eq}_{H_2}\right)^4}{p^{eq}_{SiH_4}\, p^{eq}_{CH_4} \left(p^{max}_{H_2,gas}\right)^4}$$
$$= \frac{1.59469 \times 10^{-6} \times 4.61561 \times 10^{-3} \times (0.999951)^4}{1.16175 \times 10^{-8} \times 1.64031 \times 10^{-7} \times (0.830213)^4} = 8{,}128{,}785$$

If the supersaturation ratio for deposition of silicon carbide is calculated based on (2.51),

$$\alpha_2 = \frac{p^{max}_{SiC,gas}}{p^{eq}_{SiC}} = \frac{p^{max}_{Si,gas}\, p^{max}_{C,gas}}{p^{eq}_{Si}\, p^{eq}_{C}}$$
$$= \frac{1.98744 \times 10^{-5} \times 4.29435 \times 10^{-15}}{9.98049 \times 10^{-8} \times 1.052 \times 10^{-19}} = 8{,}128{,}752$$

Therefore, the supersaturation ratio (α_1) calculated based on (2.49) is equal to that (α_2) calculated based on (2.51) within a round-off error.

2.10 Validity of the Thermodynamic Scheme

Figure 2.2 shows the CVD phase diagram of the Si–Cl–H system at 10,666 Pa and composition of N(H) = 200 and N(Cl) = 1. The line of the phase diagram divides into regions of gas and gas + solid. In the gas region, only the gas phase is stable and the solid cannot precipitate. Therefore, the supersaturation ratio for deposition should be less than unity ($\alpha < 1$). Along the line, the supersaturation ratio should be unity ($\alpha = 1$). In the gas + solid region, both gas and solid are stable and the solid can precipitate. Therefore, the supersaturation ratio should be larger than unity ($\alpha > 1$).

The supersaturation ratio, $\alpha = 1$, based on (2.42) corresponds to the phase boundary of gas/(gas + solid) in Fig. 2.2. And, the regions of $\alpha < 1$ and $\alpha > 1$ represent respectively the one-phase region of gas and the two-phase region of gas + solid. This means that the thermodynamic scheme for the supersaturation ratio for CVD given by (2.42) is valid, agreeing with the CVD phase diagram.

Equation (2.42) provides additional information in the CVD phase diagram as shown in Fig. 2.3, where the lines of iso-supersaturation ratio, $\alpha = 0.01$, $\alpha = 0.1$, $\alpha = 10$, and $\alpha = 100$ are drawn. Note that a melting point of the solid silicon is 1687 K above which the solid silicon is metastable with respect to its liquid.

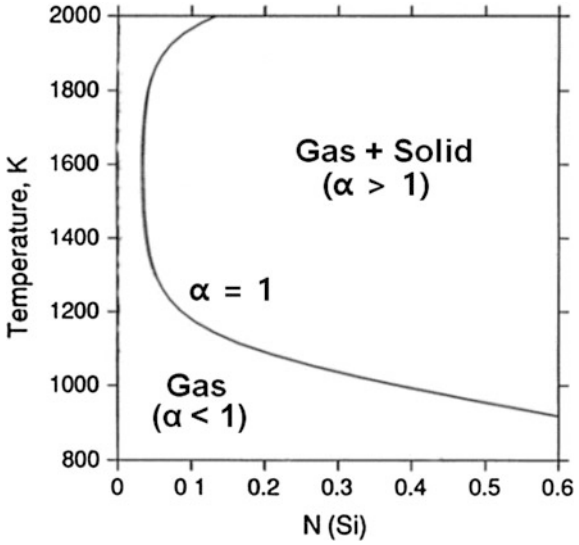

Fig. 2.2 The CVD phase diagram of the Si–Cl–H system at 10,666 Pa and composition of N(H) = 200 and N(Cl) = 1

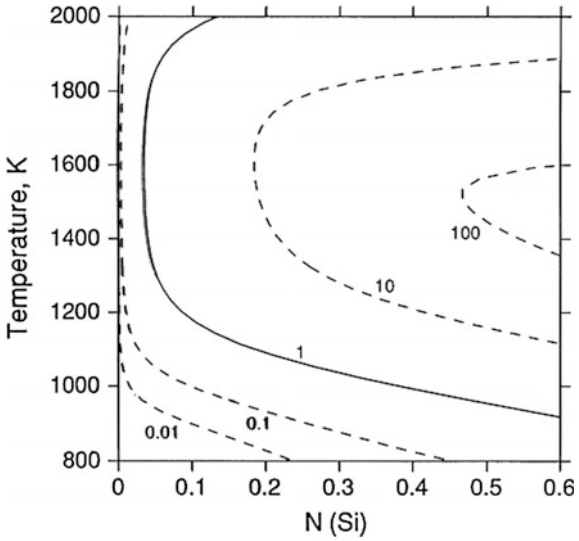

Fig. 2.3 The CVD phase diagram of the Si–Cl–H system at 10,666 Pa and composition of N(H) = 200 and N(Cl) = 1. The *dashed lines* of the iso-supersaturation ratios, 0.01, 0.1, 10 and 100 are evaluated from (2.42) (Hwang and Yoon 1994b)

Figure 2.3 shows a relatively sensitive change of the iso-supersaturation ratio with N(Si) at $\sim$1500 K, indicating the gradient of the undersaturation with N(Si) is high. By this thermodynamic scheme, lines of iso-supersaturation or driving force for etching or deposition can be evaluated with respect to any independent CVD thermodynamic variables.

2.11 Maximum Film Growth Rate in the CVD Process

Since $p_{C,gas}^{max}$ in (2.41) represents the maximum partial pressure of 'C' for the given CVD process, the flux for the maximum deposition rate can be evaluated using the Hertz-Knusen equation as

$$J_C^{max} = \frac{p_{C,gas}^{max}}{\sqrt{2\pi mkT}} \quad \text{mols/s cm}^2 \tag{2.52}$$

This equation is under the assumption that the metastable equilibrium among gas species without condensed phases is maintained at the given temperature. In order to consider the supercooling effect of the gas in the presence of the temperature gradient, $p_{C,gas}^{max}$ at the temperature, from which the gas is expected be supercooled, should be used.

Using (2.52), not only the maximum film growth rate can be estimated, but also the minimum partial pressure of the species to be deposited can be estimated if the film growth rate is given. However, in estimating the maximum film growth rate using (2.52), it is implicitly assumed that the gas phase nucleation does not occur and the film grows by individual atoms or molecules. If the gas phase nucleation occurs and thereby gas phase generated nanoparticles begin to contribute as a building block to film growth, (2.52) is not valid.

2.12 Driving Force for Deposition in the Diamond Chemical Vapour Deposition Process

One of typical processing conditions for diamond deposition by hot filament CVD (HFCVD) is the gas mixture of 1 % CH_4–99 % H_2, the reactor pressure of 2700 Pa, the substrate temperature of 1200 K and the hot filament temperature of 2300 K. By the hot filament, the reactant gases will be decomposed into many species including the solid carbon.

$$CH_4 + H_2 \rightarrow C_{gas} + CH + CH_2 + \cdots + C_{solid} \tag{2.53}$$

where C_{gas} and C_{solid} represent respectively the gas and solid carbon, which can be graphite or diamond depending on the kinetics.

The minimization of the Gibbs free energy of the mixture gas at 2700 Pa and 1200 K excluding all the condensed phases produces the metastable gas phase equilibrium which specifies each mole fraction of species as follows.

$$\Rightarrow C^* + C_2H_2^* + C_2H^* + CH_4^* + CH_3^* + C_2H_4^* + \cdots \tag{2.54}$$

where * represents the metastable gas phase equilibrium. If p_i^* is defined to represent the metastable partial pressure of the species i, p_C^* represents the maximum partial pressure of carbon that can be achieved metastably at the given thermodynamic condition.

The minimization of the Gibbs free energy excluding the stable graphite would produce the metastable equilibrium which specifies each mole fraction of species including diamond as follows.

$$\Rightarrow C^{eq,d} + C_2H_2^{eq,d} + C_2H^{eq,d} + CH_4^{eq,d} + CH_3^{eq,d} + C_2H_4^{eq,d} + \cdots + \text{diamond} \tag{2.55}$$

where all the gas species are in metastable equilibrium with diamond. Likewise, $p_C^{eq,d}$ represents the equilibrium vapour pressure of diamond at 1200 K.

The minimization of the Gibbs free energy without excluding any condensed phase would produces the stable equilibrium which specifies each mole fraction of species including graphite as follows.

$$\Rightarrow C^{eq} + C_2H_2^{eq} + C_2H^{eq} + CH_4^{eq} + CH_3^{eq} + C_2H_4^{eq} + \cdots + \text{graphite} \tag{2.56}$$

where all the gas species are in stable equilibrium with graphite. Likewise, p_C^{eq} represents the equilibrium vapour pressure of graphite at 1200 K.

Then, the maximum supersaturation ratio and driving force for graphite deposition are expressed respectively as

$$\alpha = \frac{p_C^*}{p_C^{eq}} \tag{2.57}$$

and

$$\Delta\mu^{gas\rightarrow gra} = -RT\ln\left(\frac{p_C^*}{p_C^{eq}}\right). \tag{2.58}$$

The calculation under the condition of T = 1200 K and P = 2700 Pa by Thermo-Calc (Sundman et al. 1985) based on the scientific group thermodata Europe (SGTE) substance database shows that $\alpha = 23.3$ and $\Delta\mu^{gas\rightarrow gra} = -31413$ J/mole (Hwang et al. 1994).

Similarly, the maximum supersaturation ratio and the driving force for diamond deposition are expressed as

$$\alpha = \frac{p_C^*}{p_C^{eq,d}} \tag{2.59}$$

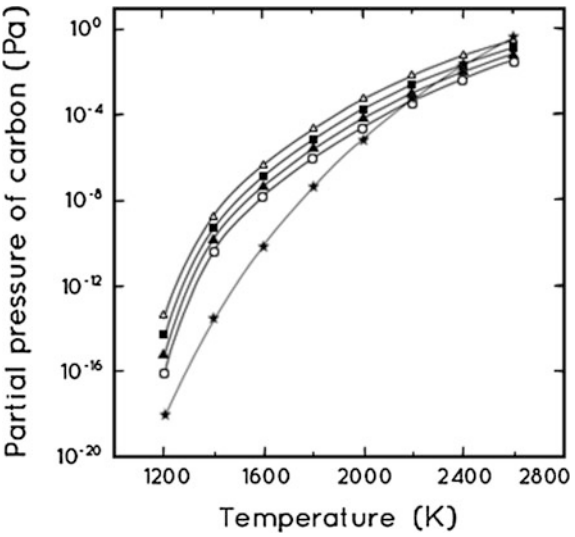

Fig. 2.4 Variation of the partial pressure of carbon in the gas phase with temperature for four different ratios of carbon to hydrogen (total pressure, 2700 Pa); Δ, C:H = 1:50; ■, C:H = 1:100; ▲, C:H = 1:200; ○,1:400; ★, equilibrium vapour pressure of graphite or diamond (Hwang et al. 1994)

$$\Delta\mu^{gas\rightarrow dia} = -RT\ln\left(\frac{p_C^*}{p_C^{eq,d}}\right) \tag{2.60}$$

The calculation shows that $\alpha = 11.7$, $\Delta\mu^{gas\rightarrow dia} = -24540$ J/mole and $\Delta\mu^{dia\rightarrow gra} = -6873$ J/mole. As seen from the supersaturation ratio, the equilibrium vapour pressure of diamond is twice larger than that of graphite. Based on this thermodynamic scheme, the metastable partial pressure of carbon can be determined with varying temperature and various mixtures of carbon and hydrogen, which is shown in Fig. 2.4 at a reactor pressure 2700 Pa. In Fig. 2.4, the equilibrium vapour pressure of graphite or diamond is also shown for comparison. It should be noted that since the vertical axis of pressure is a logarithmic scale, the slight difference in equilibrium vapour pressure between graphite and diamond is not distinguishable.

The gas mixtures of 0.5 % CH_4–99.5 % H_2, 1 % CH_4–99 % H_2, 2 % CH_4–98 % H_2 and 3 % CH_4–97 % H_2, which cover the composition range mostly used in the diamond HFCVD process, have the ratios of C to H of 1/402, 1/202, 1/102 and 1/69, respectively. For the ratio of C : H = 1 : 200, the maximum partial pressure of carbon is higher than its equilibrium vapour pressure over the temperature range between roughly 890 and 2290 K. This means that in the temperature range of $\sim$890 K < T < $\sim$2290 K, the driving force is for deposition of solid carbon and in the temperature range of T < $\sim$890 K, and T > $\sim$2290 K, the driving force is for etching of solid carbon.

This deposition condition appears to agree with the actual deposition at least to an extent. First, in the diamond HFCVD process, the deposition hardly occurs below the substrate temperature of 900 K if the gas mixture of 1 % CH_4–99 % H_2 is used. The general tendency is that the quality of diamonds is degraded when the

filament temperature decreases or the concentration of CH_4 increases. It is experimentally observed that under the condition where the solid carbon deposits on the hot filament, poor quality diamonds are formed on the substrate (Sommer et al. 1989). In order for carbon to deposit on the hot filament, the driving force should be for deposition at the hot filament temperature. Considering the above calculation, this condition is achieved when the filament temperature is decreased or the concentration of CH_4 is increased. These results indicate that in the steady state of the diamond HFCVD process, most of the reactant gases decompose.

The experimental observation that under the condition where the solid carbon deposits on the hot filament, poor quality diamonds are deposited is not a problem of thermodynamics but related with the growth mechanism of diamond. The carbon deposited filament surface can have quite a different property in its catalytic effect, which is not clearly understood. It would be better to treat this problem after the growth mechanism of diamonds is studied in Chap. 6.

From (2.60), the chemical potential of carbon in the gas can be written as

$$\mu^{gas} = \mu^{dia} + RT \ln\left(\frac{p_C^*}{p_C^{eq,d}}\right) = \mu^{dia} + RT \ln a_C^* \tag{2.61}$$

This means that if diamond is set as a reference state, the supersaturation ratio for diamond deposition becomes an activity of the gas phase. Using (2.61), the carbon activities of gas, diamond and graphite can be compared with temperature at a gas mixture of 1 % CH_4–99 % H_2 at a reactor pressure of 2700 Pa, which is shown in Fig. 2.5.

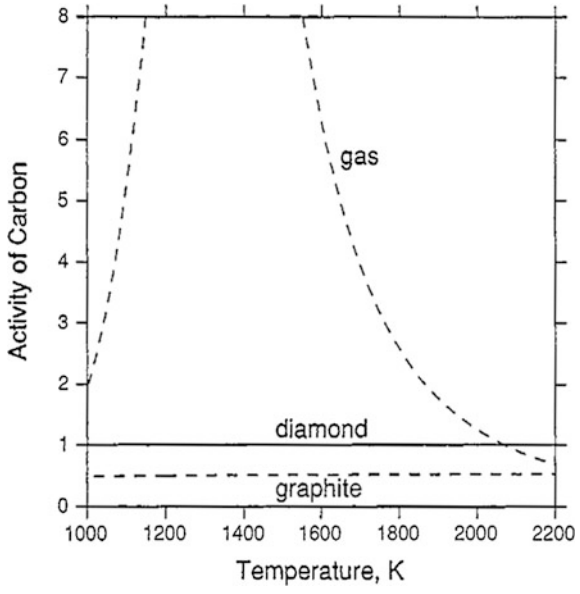

Fig. 2.5 Temperature dependence of carbon activities of gas, diamond and graphite at a gas mixture of 1 % CH_4–99 % H_2 at 2700 Pa (Hwang et al. 1996)

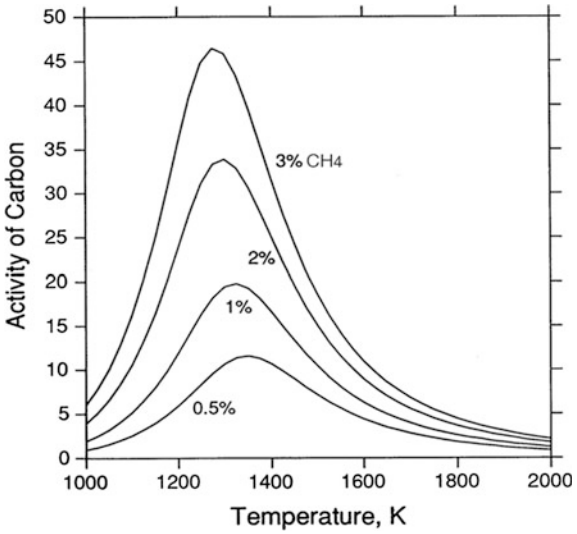

Fig. 2.6 Temperature dependence of carbon activity of gas for four different gas mixtures of 0.5 % CH_4–99.5 % H_2, 1 % CH_4–99 % H_2, 2 % CH_4–98 % H_2 and 3 % CH_4–97 % H_2 at 2700 Pa. The supersaturation ratio is with respect to graphite (Yoon and Hwang 1995)

The activity of graphite is about a half of that of diamond. The carbon activity of the gas has maximum at ~1350 K. At temperature higher than ~1350 K, the activity of the gas decreases with increasing temperature and at temperature lower than ~1350 K, it decreases with decreasing temperature. Figure 2.5 shows that the activities of gas and diamond intersect at temperature at ~2050 K, which means at temperature lower than this intersection, the driving force is for deposition of diamond and at temperature higher than this intersection, the driving force is for etching of diamond. The temperature at which the activities of gas and graphite intersect, is a little higher than 2200 K.

The carbon activity of the gas can be evaluated as a function of temperature for different concentration of CH_4 as shown in Fig. 2.6. As expected, the activity, which is the same as the supersaturation ratio for graphite deposition, increases with increasing concentration of CH_4.

Based on the thermodynamic scheme of (2.59) and (2.60), the lines of iso-supersaturation ratio or iso-activity of carbon in the gas can be calculated as a function of the atomic fraction of carbon and temperature as shown in Fig. 2.7. Since the supersaturation ratio is evaluated for diamond deposition, diamond can be deposited only in the region of $\alpha > 1$. Figure 2.7 can be divided into three regions. The first region is outside the graphite line, where only gas is stable. In this region, neither graphite nor diamond can be deposited. The second region is between the graphite and diamond lines, where graphite and gas are stable. In this region, graphite can be deposited but diamond cannot be deposited. The third region is inside the diamond line. In this region, graphite and gas are stable but diamond is metastable. In order that metastable diamond may be deposited, it is necessary that the thermodynamic condition should be in the third region. In addition to the diamond line of $\alpha = 1$, Fig. 2.7 shows other lines of $\alpha = 0.1$ and 10. Comparison of

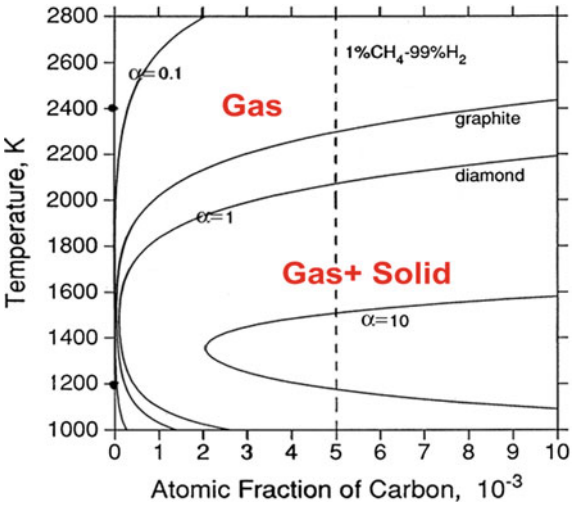

Fig. 2.7 Lines of iso-supersaturation ratio for diamond deposition as a function of temperature and atomic fraction of carbon in the C–H system (Hwang 1994)

the three lines of α = 0.1, 1 and 10 gives the information as to how steeply the supersaturation or the undersaturation varies with temperature and composition. The vertical dashed line represents the composition of 1 % CH_4–99 % H_2. At this composition, diamond deposition is possible below ~2050 K in agreement with Figs. 2.4 and 2.5.

The line of α = 1, which corresponds to the phase boundary of the CVD phase diagram, represents a solubility limit of carbon in the gas phase. In the region of α < 1, carbon is soluble in the gas phase in the form of all kinds of hydrocarbon such as CH, CH_2, and CH_3. In the region of α > 1, carbon in the gas phase exceeds the solubility limit of the gas phase and diamond can be precipitated. Figure 2.7 shows that the solubility limit is minimum at ~1350 K and increases with decreasing temperature. This increase of the solubility limit with decreasing temperature is rather an unusual case and called a retrograde solubility; normally the solubility limit decreases with decreasing temperature.

The list of commands to calculate the iso-activity lines with diamond as a reference state shown in Fig. 2.7 by Thermo-Calc is as follows. A brief explanation for each command is given.

$TC
go ges → Go to Gibbs Energy System Module
read chd → Read the data file saved with a file name of chd in the GES module
go poly-3 → Go to Poly-3 modules
"Set the thermodynamic condition so that the degree of freedom may be zero."
set-condition t = 1200 p = 2700 x(c) = 0.0049261 n = 1
→ temperature in K, pressure in Pa, the atomic fraction of carbon, x (c) = 0.0049261, corresponds to the composition of 1 % CH_4−99 % H_2, n = 1 means that the total number of mole is equal to 1.

set-automatic-starting value
Yes → accept an automatic starting value
compute-equilibrium → compute Gibbs free energy minimization for the given condition
set-reference-state c diamond → set reference state carbon as diamond
change-status phase c_s = suspend → change status of the phase solid carbon to be suspended
change-status phase graphite = suspend → change status of the phase graphite to be suspended
change-status phase diamond = suspend → change status of the phase diamond to be suspended
set-axis-value 2 t 1000 2800 → Designate y axis as temperature with its range from 1000 to 2800 K.
list-equilibrium → list the values of equilibrium calculations
TERMlNAL → Show the result on the computer terminal
VWCs
compute-equilibrium → Compute Gibbs free energy minimization for the given condition
add
set-condition X(c) = none, acr(c) = 1 → Set the constraint of the relative activity with a defined reference state being equal to 1.
compute-equilibrium → Compute Gibbs free energy minimization satisfying the constraint of the set-condition
add

The region where diamond and gas are stable in Fig. 2.7 is the two phase region, where the lever rule can be applied to determine the equilibrium amount of diamond precipitation. When the gas mixture of 1 % CH_4–99 % H_2 is used, the atomic fraction of 1 % CH_4–99 % H_2 is 5×10^{-3} as shown by the vertical dashed line in Fig. 2.7. If the minimum carbon solubility is 10^{-4} at ~1350 K, the mole fraction of diamond can be determined by the lever rule as

$$\text{Mole fraction of diamond} = \frac{5 \times 10^{-3} - 10^{-4}}{1 - 10^{-4}} = 0.0049 \tag{2.62}$$

Then, the mole fraction of gas is 1 − 0.0049 = 0.9951. Since the mole fraction of diamond is evaluated at the minimum solubility of carbon at ~1350 K, this mole fraction is maximum and would decrease with decreasing temperature.

This decrease in the amount of precipitation with decreasing temperature is a unique feature of the retrograde solubility. This fact has a very special meaning in the deposition of diamond and silicon by HFCVD, where the temperature decreases monotonously from the hot filament to the substrate. In such cases, if the gas phase nucleation takes place, the equilibrium amount of gas phase nuclei would decrease toward the substrate temperature, considering the temperature gradient. This means

that in the presence of gas phase nuclei, the driving force is for etching at the substrate temperature.

If any film grows on the substrate in this situation, it can be inferred that the film grow by the gas phase nuclei because the driving force is for etching. In other words, the gas phase nuclei deposit on the substrate as a film and simultaneously the deposited film would undergo etching atomically. Simultaneous deposition and etching are often macroscopically observed in the CVD process (Badzian et al. 1988; Salvadori et al. 1992; Kumomi and Yonehara 1990). This phenomenon provides the indirect evidence that the film should grow 100 % by gas phase nuclei because atomic contribution is negative by etching. This aspect will be explained in more detail in Chaps. 6 and 7.

If the gas phase nucleation takes place, which turns out to be very general in the thin film process by CVD or even by some PVD, the information about the equilibrium amount of precipitation is important because this amount is related with the deposition rate. Figure 2.8 shows the temperature dependence of the equilibrium amounts of diamond and graphite that can be precipitated from the gas phase when the gas mixture of 1 % CH_4–99 % H_2 is used at the reactor pressure of 2700 Pa (Hwang and Yoon 1996). In the entire range of temperature, the equilibrium fraction of graphite is larger than that of diamond in agreement with the fact that graphite is more stable than diamond.

Figure 2.8 provides an important fact that the equilibrium amount of diamond to be precipitated in the gas phase decreases with decreasing temperature, which can explain the well-known but extremely puzzling experimental observation of simultaneous diamond deposition and graphite etching in the diamond CVD process.

The reactor pressure is an important process parameter. What would be the effect of pressure on the C–H phase diagram? As mentioned earlier, the line of $\alpha = 1$

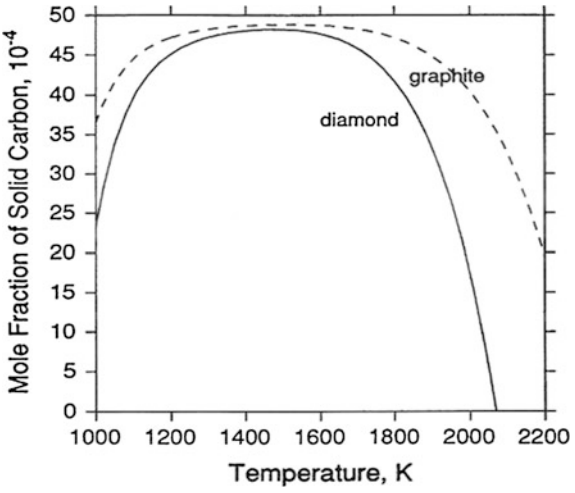

Fig. 2.8 The temperature dependence of the equilibrium mole fraction of diamond and graphite when the gas mixture of 1 % CH_4–99 % H_2 is used at 2700 Pa. The *dashed* and *solid lines* are for graphite and diamond, respectively (Hwang and Yoon 1996)

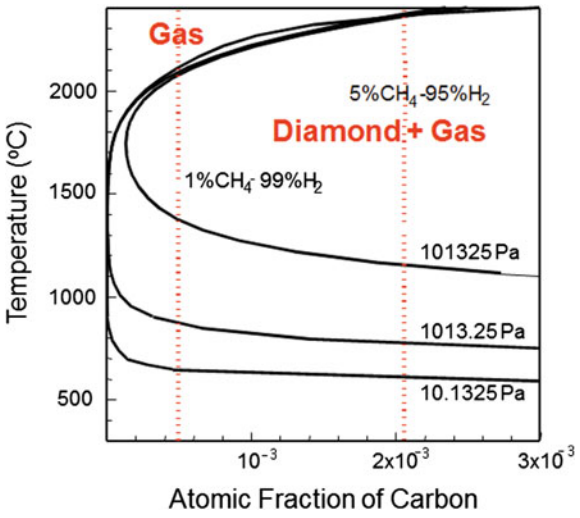

Fig. 2.9 Metastable CVD phase diagram of the C–H system: in the *left* of the curve, only a gas phase is stable and in the *right* of the curve, two phases of gas + diamond are stable (Gueroudji and Hwang 2000)

corresponds to the phase diagram, which represents the thermodynamic limit of deposition. In the C–H system using a gas mixture of CH_4 and H_2, it is known that there is a lower limit of the substrate temperature that diamond can be deposited and this temperature increases with increasing reactor pressure. The effect of the pressure on the line of $\alpha = 1$ or the metastable diamond CVD phase diagram is shown in Fig. 2.9, which divides the region into the gas phase and the gas + diamond phase (Gueroudji and Hwang 2000). The curves drawn in Fig. 2.9 correspond to the temperature dependence of the solubility limit of carbon separating a diamond deposition domain from its etching or non-deposition domain at different values of the total pressure in the system.

At 101,325 Pa for a gas mixture of 1 % CH_4–99 % H_2 indicated by the left vertical dashed line in Fig. 2.9, the lower limit of temperature for diamond deposition is $\sim$1400 K. It should be noted that the substrate temperature cannot be increased too much because diamond starts to transform to graphite. This temperature is $\sim$1500 K, which would be the practical upper limit of the deposition temperature. With increasing the methane concentration to 5 % CH_4–95 % H_2 indicated by the right vertical dashed line in Fig. 2.9, the deposition domain can be extended and the lower limit is $\sim$1200 K. In experimental reality, however, increasing the methane concentration tends to degrade the quality of diamond or to produce the non-diamond phase. Normally, the methane concentration in typical conditions is less than 3 % in the C–H system. Figure 2.9 shows that the lower limit of the substrate temperature for diamond deposition can go down to $\sim$900 K at 1013.25 Pa and $\sim$600 K at 10.1325 Pa for the gas mixture of 1 % CH_4–99 % H_2. However, the reactor pressure cannot be reduced much in the HFCVD process because the evaporation rate of tungsten hot filaments increases, which will degrade the diamond film quality.

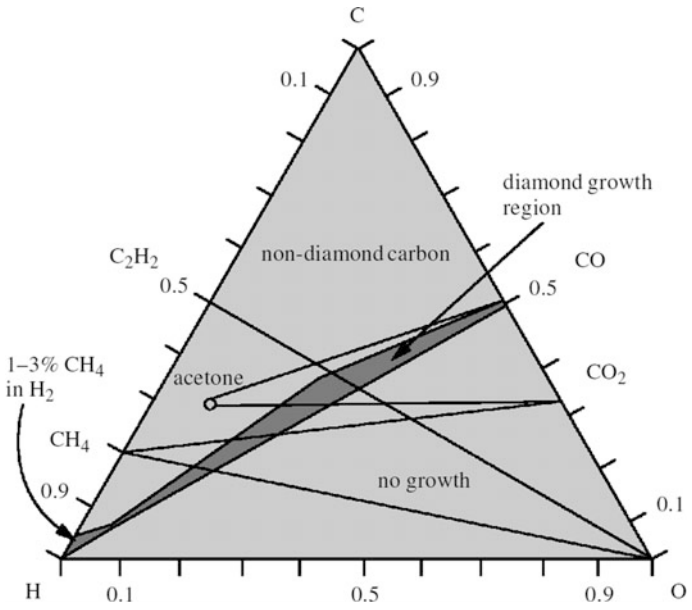

Fig. 2.10 A simplified form of the Bachmann C–H–O diagram for diamond deposition. Below the H–CO tie line, no growth was achieved. Above the H–CO tie line, non-diamond carbon is generally deposited except in a narrow window close to the tie line, which produces polycrystalline diamond (May 2000)

The gas mixture of CH_4 and H_2 is just one example to deposit diamond. It turned out that various sources can be used to deposit diamond. For examples, not only pure methanol and pure acetone, but various gas mixtures containing carbon, hydrogen, and oxygen such as CH_4–H_2–O_2, CH_4–H_2–H_2O, CH_4–CO–H_2, CH_4–CO_2–H_2, CO–H_2, C_2H_2–O_2, C_2H_4–O_2, C_2H_6–O_2, C_2H_2–CO_2, C_2H_2–O_2–H_2, C_2H_2–O_2–H_2, CH_3COCH_3–H_2, CH_3COCH_3–O_2, CH_4–CH_3COCH_3–O_2, CO–CO_2–H_2, and CO–H_2–O_2. Besides, in addition to HFCVD, various CVD processes such as microwave plasma, DC plasma jet, and flame could be used. By examining vast compiled reports on diamond CVD, Bachmann et al. (1991) found out that the diamond deposition is highly correlated with some composition range in the C–H–O system regardless of the sources of reactants nor the method of processes. Diamond deposition was possible only in the narrow composition range centred at the ratio of C/O = 1 with varying hydrogen in the C–H–O system. In the carbon-rich side of the line of C/O = 1, non-diamond is generally deposited and in the oxygen-rich side, there was no growth. This aspect is shown in Fig. 2.10.

There must be some reason behind this high correlation of the diamond deposition behaviour with the specific composition range. Before going further, it is worth thinking why this is so.

(Q) What do you think is the reason for this deposition behaviour?

Among the possibility we can think of, the thermodynamics should come first. In other words, this deposition behaviour might be related with the thermodynamic driving force for diamond deposition. If the thermodynamic scheme for the supersaturation ratio for diamond deposition given in (2.59) is applied, the lines of iso-supersaturation ratio can be evaluated at 1200 K in the C–H–O system as shown in Fig. 2.11.

The supersaturation ratio for diamond deposition is unity almost along the line of C/O = 1. In the carbon-rich side of this line, the supersaturation ratio increases steeply with increasing carbon. This tendency is strong especially when the hydrogen content is small. In the oxygen-rich side, the supersaturation ratio is less than unity and the driving force is for etching of diamond. If Fig. 2.11 is compared with Fig. 2.10, the diamond deposition behaviour is related with the supersaturation ratio. No growth in the oxygen-rich side of the line of C/O = 1 might be related with the supersaturation ratio being less than unity. In other words, this region is undersaturated and the driving force is for etching of diamond. And non-diamond deposition is related with the high supersaturation ratio. It may be asked why non-diamond deposits under the condition of the high supersaturation ratio. This problem is related with the diamond deposition mechanism, which will be explained in Chap. 6.

The thermodynamic analysis made so far shows that the diamond deposition is thermodynamically sound in that diamond deposition occurs under the thermodynamic condition where the driving force is for deposition of diamond. The deposition of less stable diamond instead of stable graphite is not a problem of thermodynamics but a problem of kinetics, which will be explained in Chap. 5.

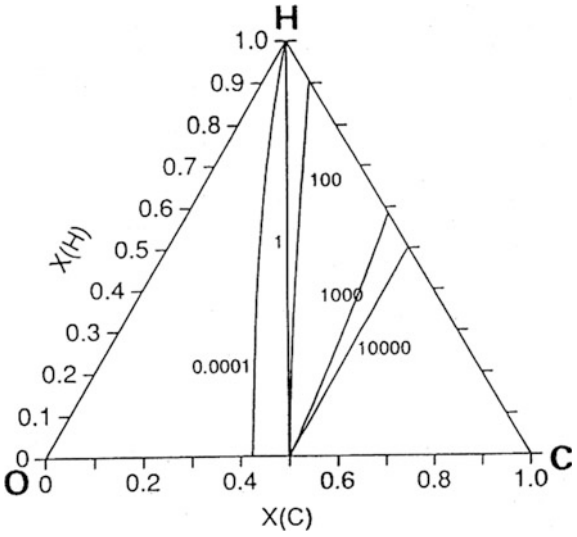

Fig. 2.11 The ternary composition diagram of the C–H–O system at 1200 K under 2700 Pa showing five different *lines* of the iso-supersaturation ratio for diamond deposition (Hwang 1994)

2.13 Kinetics

The important thermodynamic functions such as E (internal energy), H (enthalpy), G (Gibbs free energy), and S (entropy) are state functions, which does not depend on the path. The information about two out of the three state variables P, T and V is enough to determine these state functions. For example, if P and T are known for states A and B, the Gibbs free energy, G, for each state can be determined. Then, we can determine the direction of irreversibility or whether A → B or B → A. If $G_A > G_B$, the state A irreversibly changes to the state B and vice versa. This is illustrated in Fig. 2.12.

Although thermodynamics can powerfully predict the direction of irreversibility of A → B from the knowledge of $G_A > G_B$, it does not say anything about how long it will take for state A to change to state B. Time is not a parameter in thermodynamics. How long the process will take is not a problem of thermodynamics but a problem of kinetics.

(Q) If thermodynamics allows the irreversibility of A → B as shown in Fig. 2.12a and the process is thermally activated, what would be the factors that determine the rate?

The important factor is the kinetic barrier for the process A → B. If the kinetic barrier is ΔG^*, the probability to overcome the kinetic barrier would be identical to the Boltzman probability for the thermally-activated process. Therefore, the probability would be proportional to $\exp(-\Delta G^*/kT)$.

There is a case where there exist multiple kinetic paths. For example, consider the situation where $G_A > G_B > G_C$. In this case, nature has two choices, either A → B or A → C.

(Q) In this case, which path will nature choose, A → B or A → C?

Since $G_A > G_B > G_C$, the magnitude of $\Delta G_{A\to C}$ is larger than that of $\Delta G_{A\to B}$. Does this mean that nature chooses the path A → C instead of the path A → B? Thermodynamics does not say anything about this possibility. Larger driving force does not guarantee faster kinetics. The determining factor is the kinetic barrier. If the kinetic barrier of the A → B path is smaller than that of the A → C path, nature will choose the path of A → B. In this sense, it can be said that nature

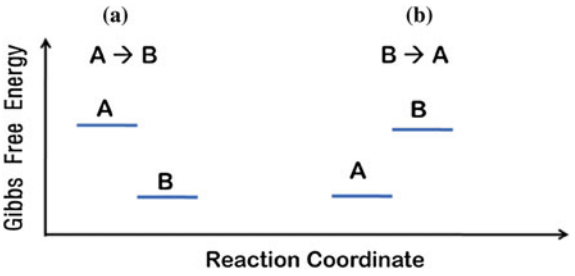

Fig. 2.12 The direction of irreversibility of **a** A → B or **b** B → A is determined by the relative magnitude of Gibbs free energy at constant temperature and pressure

proceeds in the most probable way. This kinetic law can be compared with the second law of thermodynamics, which says that nature does not proceed in a less probable way.

The kinetic statement that nature proceeds in the most probable way exactly describes what nature does whereas the thermodynamic statement that nature does not proceed in a less probable way rather vaguely describes what nature does. For the nature's way of doing, the kinetic statement provides a necessary and sufficient condition but the thermodynamic statement provides a necessary condition. Considering this, the kinetic statement sounds much more attractive and powerful than the thermodynamic one.

(Q) Then, why do we bother to learn thermodynamics? What is the advantage of thermodynamics over kinetics?

The advantage of thermodynamics lies in the fact that important thermodynamic functions are a state function, which makes thermodynamics very simple, powerful and generally formulated. This is why we bother to learn thermodynamics, which is worth our laborious efforts. This is highly in contrast with kinetics which depends on the path. This means that there is no general way to formulate the kinetics. This is why the general formulation for kinetics is not available and each kinetics should be approached case by case.

References

Bachmann PK, Leers D, Lydtin H (1991) Towards a general concept of diamond chemical vapour deposition. Diam Relat Mater 1(1):1–12. doi:10.1016/0925-9635(91)90005-U

Badzian AR, Badzian T, Roy R, Messier R, Spear K (1988) Crystallization of diamond crystals and films by microwave assisted CVD (Part II). Mater Res Bull 23(4):531–548

Gaskell DR (1995) Introduction to the thermodynamics of materials. Taylor & Francis, Washington, DC

Gueroudji L, Hwang NM (2000) Thermodynamic limits for the substrate temperature in the CVD diamond process. Diam Relat Mater 9(2):205–211. doi:http://dx.doi.org/10.1016/S0925-9635(00)00232-6

Hillert M, Aaronson H (1975) Lectures on the theory of phase transformations. Amer Inst Mining, Metallurgical and Petroleum Engrs, New York, p 1–44

Hwang NM (1994) Thermodynamic analysis of the chemical vapor deposition of diamond in the C-H, C-O and C-H-O systems. J Cryst Growth 135(1):165–171. doi:http://dx.doi.org/10.1016/0022-0248(94)90738-2

Hwang N, Yoon D (1994a) Driving force for deposition in the chemical vapour deposition process. J Mater Sci Lett 13(19):1437–1439

Hwang NM, Yoon DY (1994b) Thermodynamic approach to the chemical vapor deposition process. J Cryst Growth 143(1–2):103–sss109. doi:10.1016/0022-0248(94)90372-7

Hwang NM, Yoon DY (1996) Thermodynamic approach to the paradox of diamond formation with simultaneous graphite etching in the low pressure synthesis of diamond. J Cryst Growth 160(1–2):98–103. doi:http://dx.doi.org/10.1016/0022-0248(95)00549-8

Hwang NM, Hahn JH, Bahng GW (1994) Thermodynamic approach to the C–H–O deposition diagram in the diamond chemical vapour deposition process. Diam Relat Mater 3(1–2):163–167. doi:http://dx.doi.org/10.1016/0925-9635(94)90051-5

Hwang NM, Hahn JH, Yoon DY (1996) Chemical potential of carbon in the low pressure synthesis of diamond. J Cryst Growth 160(1–2):87–97. doi:http://dx.doi.org/10.1016/0022-0248(95)00548-X

Kumomi H, Yonehara T (1990) Coarsening phenomenon of Si clusters. In: MRS Proceedings, Cambridge Univ Press, p 83

May PW (2000) Diamond thin films: a 21st-century material. Phil Trans R Soc A 358(1766):473–495

Salvadori M, Brewer M, Ager J, Krishnan K, Brown I (1992) The effect of a graphite holder on diamond synthesis by microwave plasma chemical vapor deposition. J Electrochem Soc 139 (2):558–560. doi:10.1149/1.2069256

Sommer M, Mui K, Smith FW (1989) Thermodynamic analysis of the chemical vapor deposition of diamond films. Solid State Commun 69(7):775–778. doi:http://dx.doi.org/10.1016/0038-1098(89)90829-6

Sundman B, Jansson B, Andersson J-O (1985) The thermo-calc databank system. Calphad 9(2):153–190. doi:http://dx.doi.org/10.1016/0364-5916(85)90021-5

Yoon DY, Hwang NM (1995) Thin film fabrications: thermodynamics of chemical vapor deposition and its application to diamond deposition. Adv Mater Proc 1:905–911

http://www.springer.com/978-94-017-7614-1

Non-Classical Crystallization of Thin Films and Nanostructures in CVD and PVD Processes

Hwang, N.M.

2016, XII, 332 p. 229 illus., 64 illus. in color., Hardcover
ISBN: 978-94-017-7614-1